SIMULATIONS OF TIME-DEPENDENT NEUTRON SCATTERING IN LAYERED MATERIALS CONTAINING HYDRATED MINERALS. C. Hardgrove[1], J. E. Moersch[1], R. Starr[2], T. McClanahan[2] and A. Parsons[2], [1]University of Tennessee (Department of Earth and Planetary Sciences, University of Tennessee, Knoxville, TN, 37996) [2]NASA Goddard Space Flight Center (Greenbelt, MD) [1]University of Tennessee (Department of Earth and Planetary Sciences, University of Tennessee, Knoxville, TN, 37996)

Introduction: The Dynamic Albedo of Neutrons (DAN) instrument, to be included on-board the Mars Science Laboratory (MSL) rover, will quantify the hydrogen abundance and stratigraphy as it traverses the surface of Mars [1]. After a pulse of high energy (14 MeV) neutrons is fired into the surface, the DAN instrument will detect those neutrons that have interacted with materials from within the subsurface (< ~0.5 m deep) and scattered back toward the detectors. When binned by time, the flux of neutrons arriving at the detector will be a function of the amount of hydrogen and the stratigraphy of hydrogen-rich materials within the subsurface. Early studies [2], and recent experimental and modeling results [1, 3, 4] have confirmed that neutron die-away curves acquired from DAN will be sensitive to hydrogen-content of the near-subsurface, the depth of a buried hydrogen-rich layer and possibly buried phyllosilicates. These results reveal the potential of the Dynamic Albedo of Neutrons (DAN) instrument on-board the Mars Science Laboratory (MSL) rover to identify local regions within the subsurface with increased amounts of hydrogen as it moves across the Martian surface.

It is often assumed that the hydrogen detected is present in water or ice in the near-surface, however, neutrons will be moderated by any material that contains hydrogen in even moderate quantities (100 ppm) [5]. Hydrated minerals, which can contain hydrogen in abundances well over 100 ppm, have been detected by several spacecraft missions in a variety of locations on Mars [6, 7, 8]. These minerals not only contain significant quantities of hydrogen, they also can contain elements such as iron (*e.g.* jarosite) and chlorine (*e.g.* apatite) which both have high thermal neutron absorption cross sections. It is therefore important to not only understand the effects of increased hydrogen abundances in these minerals, but also the secondary effects from abundances of high thermal neutron absorption cross section elements. We first extend the modeling efforts by [3] to include a larger suite of hydrated minerals. We also do not confine the hydrated minerals to discrete layers, instead, all material below each depth contains the hydrated mineral. In addition, we vary the mixing ratios between regolith, water-ice and the hydrated minerals themselves to determine their detectability by DAN.

Methods: We use the Monte Carlo Neutral Particle eXtended code (MCNPX) to model neutron scattering in the subsurface. Our modeled detectors are similar to those used with DAN, two 15 cm long He-3 neutron detector tubes, with one tube wrapped in a 0.02 cm thick coating of cadmium to filter thermal neutrons. We use a neutron source with a gaussian fusion distribution peaked at 14.0 MeV with a deuterium-tritium target. The neutron source and detector tubes are both positioned 10 cm above the surface. For regolith composition, we use a standard Surface Type 1 (ST1) mineralogy [9]. [10] used Mars Odyssey Gamma-Ray Spectrometer elemental data to estimate upper-limits for the abundances of hydrated minerals (between 2 and 30 wt. %) at several locations on Mars, while [8] estimate as high as 45 wt. % for gypsum based on spectral data from Mars Reconnaissance Orbiter (MRO). Using their estimates, we model a range of proportions from 10 - 50 wt. % for each hydrated mineral. For each model run, we are only considering one hydrated mineral mixed with ST1. We select our hydrated minerals from [8], who compiled visible and infrared spectral data from the first Mars year of MRO data to form a catalog of hydrated mineral classes and their associated locations on Mars. Filtering their list by those regions that could plausibly be accessed by MSL, we compile a list of minerals that can be readily modeled in MCNPX. These minerals, as described by [8], are found in intracrater fans and plains sediments (Fe/Mg smectites), intracrater clay-sulfate deposits (kaolinite, hydrated sulfates, alunite, jarosite), Meridiani-type layered deposits (hydrated sulfates, jarosites), siliceous layered deposits (hydrated silica, opal, jarosite) and the gypsum plains (gypsum).

For layering (Figure 1), we model the subsurface with discrete intervals between 5 - 15 cm, 15 - 40 cm, 40 - 90 cm, and 90 cm - 100 meters, with the first layer from 0-5 cm fixed as a dry (~2% water mass fraction) ST1 material. For simple hydrated mineral models (Figs. 2 and 3) we model one homogeneous layer of each mineral below 5 cm to determine if end-member (pure) cases are distinguishable. We then mix these end-members with ST1 (again in one homogeneous layer below 5 cm) in varying proportions to determine if they remain detectable, and at what proportions they are not distinguishable from ST1.

Results: Our simple model for an artificially hydrated ST1 layer at various burial depths is in qualitative agreement with [3], with increases in neutron counts between 300 - 460 μs after the start of the pulse

(Figure 1). The initial decrease in neutron flux in all figures represents the trailing edge of the source pulse, which was 200 μs in duration. The inflection points in Figure 1, labeled with arrows, are superimposed on the overall neutron die-away and represent a time-dependent increase in neutron counts greater than the natural die-away from the pulse, which is due to buried hydrogen-rich layers. The inflection points labeled in Figure 1 for the buried 25% hydrated layer at 5 cm and 15 cm match the results of [3], while the results for layers below 40 cm are consistent with the stated inability to distinguish layers below ~50 cm. Figure 2 shows the results for five phyllosilicate minerals, an Fe-nontronite (FeN), jarosite, kaolinite, gypsum and opal. Epithermal neutron counts are elevated for minerals that are more rich in hydrogen, with the exception of jarosite and kaolinite. The high iron content (~32 wt. %) in jarosite initially elevates the epithermal neutron flux by moderating fast neutrons, however, because jarosite only contains ~1 wt. % hydrogen the epithermal neutron flux drops off rapidly. Kaolinite and FeN are not statistically different, despite a moderate difference in hydrogen content. Although FeN contains a significant amount of iron (20 wt. %), it has very little hydrogen (~0.4 wt. %), which is not enough to elevate the epithermal neutron flux. Kaolinite has only a modest amount of hydrogen (~1.5 wt. %), which although more than FeN, kaolinite also contains no iron to moderate fast neutrons.

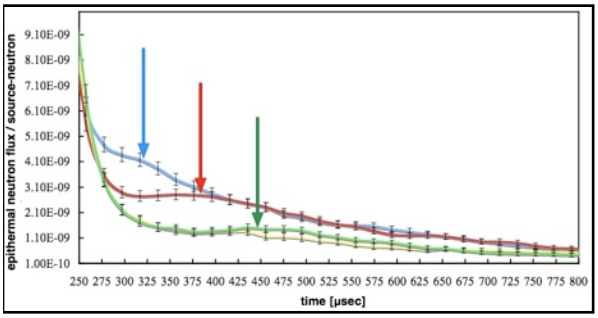

Figure 1: *Time-dependent epithermal neutron flux (per source neutron) for four burial depths of a 25 wt. % hydrogen-rich ST1 layer; 5 cm (blue), 15 cm (red), 40 cm (green), 90 cm (yellow). Colored arrows indicate secondary inflection point times, which represent an increase in neutron flux at that time. These times qualitatively match the pulse height maxima identified by Litvak et al. for similar scenarios [2]. At 5 cm depth (blue line) the inflection point lies at 318 μs, at 15 cm depth (red line) the inflection point lies at 380 μs and at 40 and 90 cm (green and yellow lines) the inflection point lies at 460 μs. Maximum relative error is ~9%.*

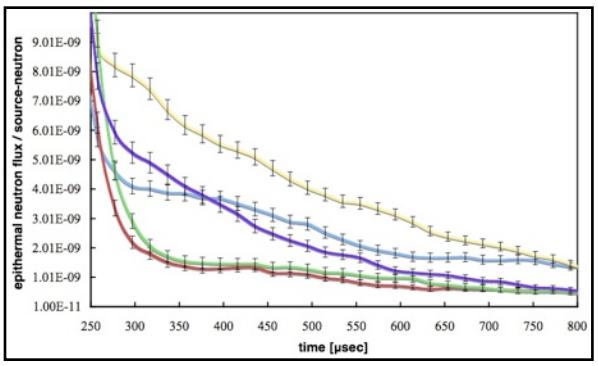

Figure 2: *Time-dependent epithermal neutron flux for five hydrated minerals buried at 5cm depth; FeN ~0.4 wt. % H (green), Jarosite ~1 wt. % H (purple), Kaolinite ~1.5 wt. % H (red), Gypsum ~2 wt. % H (blue), and Opal ~4 wt. % H (yellow). The time-dependent flux is elevated for minerals with greater wt. % H, however, jarosite, with ~32 wt. % iron and only ~1 wt. % H, shows an initially elevated flux that drops off more rapidly than others. Maximum relative error is ~13%.*

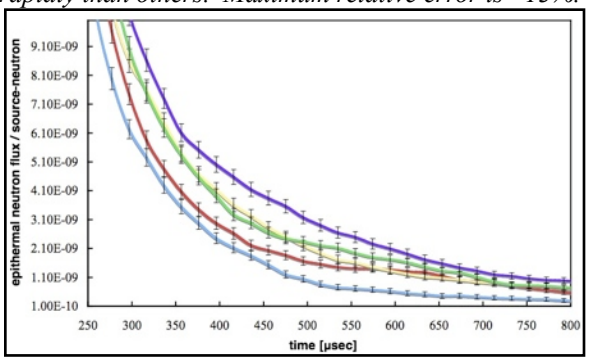

Figure 3: *Time-dependent epithermal neutron flux for several mixed proportions of FeN and ST1 layer; 100% ST1 (blue), 80% ST1 - 20% FeN (red), 70% ST1 - 30% FeN (green), 60% ST1 - 40% FeN (yellow), 50% ST1 - 50% FeN (purple). Maximum relative error is ~15%.*

Conclusions: Initial results for several hydrated minerals show that time-dependent neutron data can reveal differences between mineralogies of varying hydration states and iron content (Fig. 2). Figure 3 shows that by mixing ST1 regolith with a hydrated silicate (FeN), statistically significant differences in the rate of neutron die-away are observed. Our results suggest that distinguishing not only differences in hydrogen abundance but mineralogic diversities will allow DAN to aid in geologic interpretations.

References: [1] Litvak et al. (2008) *Astrobio., 8, 3*. [2] Trombka et al. (1963) Analysis Instr. [3] Litvak et al. (2009) *LPSC XXXX #1250*. [4] Litvak et al. (2007) LPSC XXXVIII #1554 [5] Mitrofanov, et al. (2003) Solar Sys. Res. 37:366–377. [6] Bibring et al. (2005) Science 307. [7] Poulet et al. (2005) Nature 438. [8] Murchie, S.L. (2009) JGR, 114. [9] Wyatt, M.B. & McSween H.Y. (2002) Nature 417. [10] Mitrofanov, et al. (2008) *LPSC XXXIX #1597*.